

Communication

5,8-Di-*tert*-butyl-2-hydroxy-1*H*-benzo[de]isoquinoline-1,3(2*H*)-dione—A New Lipophilic *N*-oxyl Radical Precursor

Elena R. Lopat'eva ¹, Artem D. Kutykov ^{1,2}, Igor B. Krylov ^{1,*} and Alexander O. Terent'ev ^{1,*}

¹ N. D. Zelinsky Institute of Organic Chemistry, Russian Academy of Sciences, 47 Leninsky Prospekt, Moscow 119991, Russia

² Faculty of Chemistry, Moscow State University, 1-3 Leninskiye Gory, Moscow 119991, Russia

* Correspondence: krylovigor@yandex.ru (I.B.K.); terentev@ioc.ac.ru (A.O.T.)

Abstract: *N*-hydroxyimides are widely known as organocatalysts for aerobic oxidation and oxidative coupling reactions, in which corresponding imide-*N*-oxyl radicals play the role of catalytically active hydrogen atom abstracting species. The drawbacks of many *N*-hydroxyimides are poor solubility in low polarity solvents and limited activity in the cleavage of unactivated C–H bonds. To overcome these shortcomings, we have synthesized a new lipophilic *N*-hydroxyimide, 5,8-di-*tert*-butyl-2-hydroxy-1*H*-benzo[de]isoquinoline-1,3(2*H*)-dione, with high solubility in low-polarity solvents such as DCM. According to the EPR study, the stability of the corresponding imide-*N*-oxyl radical is comparable to that of the non-*tert*-butylated analogue, naphthalimide-*N*-oxyl radical. DFT calculations showed that the NO–H bond dissociation enthalpy (BDE) in the synthesized *tert*-butylated-*N*-hydroxynaphthalimide is one of the highest in *N*-hydroxyimide series, which corresponds to high hydrogen atom abstracting reactivity and may be useful in catalysis of strong C–H bond oxidative cleavage. The synthesized compound can be considered as catalyst for liquid-phase free-radical oxidation and oxidative coupling reactions in non-polar media where solubility was previously the limiting factor.

Keywords: *N*-hydroxyimides; *N*-hydroxynaphthalimide; imide-*N*-oxyl radicals; free radical oxidation; organocatalysis



Citation: Lopat'eva, E.R.; Kutykov, A.D.; Krylov, I.B.; Terent'ev, A.O. 5,8-Di-*tert*-butyl-2-hydroxy-1*H*-benzo[de]isoquinoline-1,3(2*H*)-dione—A New Lipophilic *N*-oxyl Radical Precursor. *Molbank* **2023**, *2023*, M1543. <https://doi.org/10.3390/M1543>

Academic Editors: Maria Luisa Di Gioia, Luisa Margarida Martins and Isidro M. Pastor

Received: 30 November 2022

Revised: 17 December 2022

Accepted: 6 January 2023

Published: 11 January 2023



Copyright: © 2023 by the authors. Licensee MDPI, Basel, Switzerland. This article is an open access article distributed under the terms and conditions of the Creative Commons Attribution (CC BY) license (<https://creativecommons.org/licenses/by/4.0/>).

1. Introduction

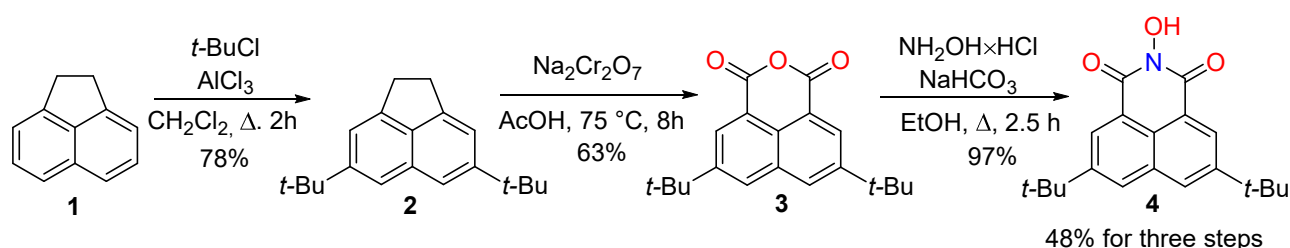
N-hydroxyimides are widely applied as redox organocatalysts [1–7] and reagents for free-radical C–O coupling [8–15]. The well-known example is *N*-hydroxyphthalimide (NHPI): it is synthetically available on an industrial scale, and it is one of the best organocatalysts for the liquid phase aerobic free-radical oxidation of hydrocarbons [1–7]. *N*-hydroxyimides are also widely used as organocatalysts or reagents in oxidative coupling reactions with the formation of C–C [16] and C–heteroatom bonds [8–17], and as reagents for the oxidative difunctionalization of alkenes [18–20]. One of the significant drawbacks of NHPI is its low solubility in low-polarity solvents (DCE, PhH, alkanes), which limits its use in some cases [21–23]. On the other hand, there is a long-standing goal to develop novel *N*-hydroxycompounds as precursors of *N*-oxyl radicals with different levels of hydrogen atom abstracting ability [24] in order to achieve optimal catalytic efficiency and selectivity for various types of substrates for CH-functionalization [1,25]. As a rule, the stability of a free radical to self-decay drops with the increase of its hydrogen atom abstracting properties. Thus, it is an especially challenging task to find *N*-hydroxycompound with high hydrogen atom abstracting activity (corresponding to high NO–H bond dissociation enthalpy, BDE), and relatively high stability to self-decay making effective catalytic turnover possible. Several catalytically effective lipophilic NHPI derivatives were reported [21–23]. However, BDE values for these derivatives were very close to that of parent NHPI [23]. *N*-hydroxynaphthalimide (NHNI) is believed to have a significantly higher (ca. 6 kcal/mol)

NO-H BDE compared to NHPI according to the DFT calculations [26]. This implies the higher reactivity of the naphthalimide-*N*-oxyl radical towards H-atom abstraction from the inert C-H bonds. However, NHNI has even lower solubility in non-polar solvents compared to NHPI, which significantly limits its use. Therefore, the synthesis of a lipophilic analogue based on NHNI is of great interest for the catalytic oxidation of strong C-H bonds in such substrates as alkanes. NHNI presents the only known *N*-oxyl radical precursor with naphthalimide moiety and its catalytic properties were poorly studied [3,17,26–28]. There are a few examples showing that NHNI can act as a coupling partner in oxidative C-O coupling reactions [8,13], although the yields are generally low and may suffer from the low solubility of NHNI. Thus, the aim of this work was to synthesize a lipophilic NHNI derivative and study its ability to be a precursor of *N*-oxyl radicals—important catalytically active intermediates in *N*-hydroxyimide-catalyzed oxidative processes.

2. Results

2.1. Synthesis of 5,8-Di-*tert*-butyl-2-hydroxy-1*H*-benzo[de]isoquinoline-1,3(2*H*)-dione

To enhance the lipophilicity of the molecule and its solubility in organic medium it is desirable to introduce lipophilic functional groups, such as long alkyl or *tert*-butyl. Considering the application of *N*-hydroxyimides in free-radical oxidative processes catalysis it is also important to avoid fragments sensitive to oxidation (such as benzylic C-H bonds). Thus, we modified the NHNI structure with *tert*-butyl groups to obtain the lipophilic *N*-hydroxyimide **4**, which is highly soluble in non-polar solvents (Scheme 1).



Scheme 1. Synthetic strategy for the preparation of 5,8-di-*tert*-butyl-2-hydroxy-1*H*-benzo[de]isoquinoline-1,3(2*H*)-dione **4**.

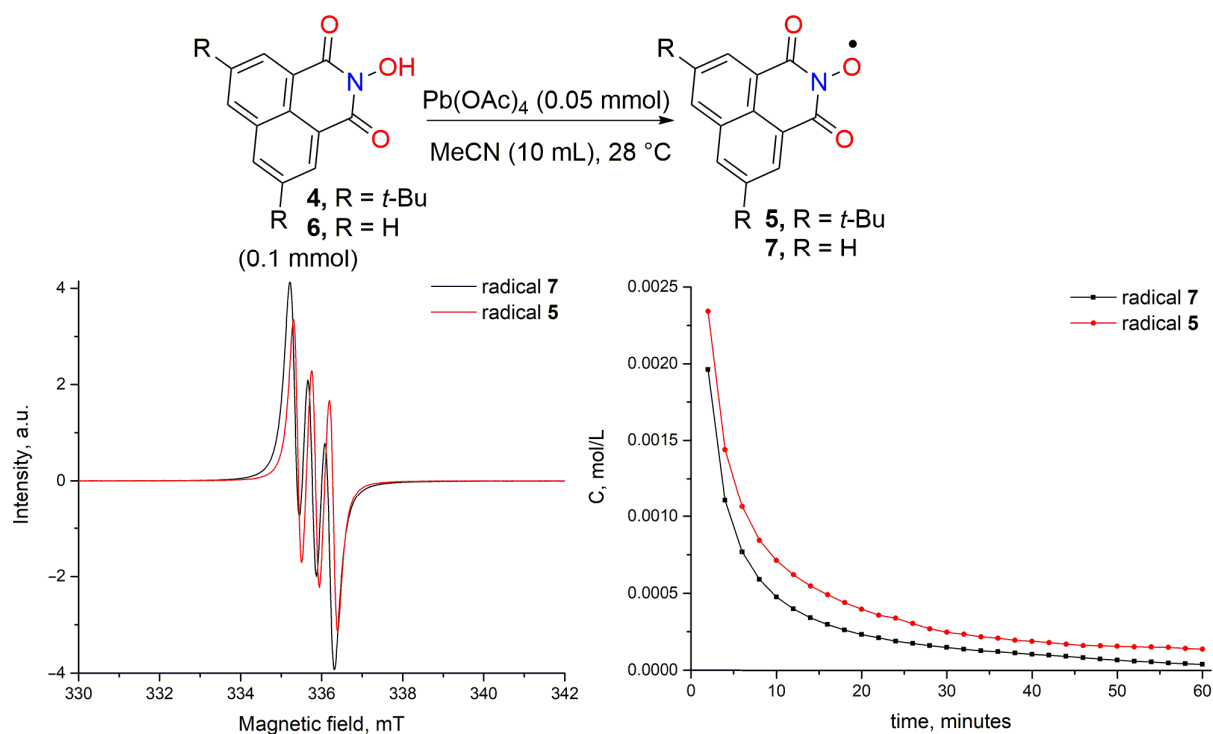
The industrially available acenaphthene **1** was chosen as the starting compound, for which the selective alkylation reaction at positions 4 and 7 is known [29]. Using two equivalents of *tert*-butyl chloride under standard Friedel–Crafts alkylation conditions, 4,7-di-*tert*-butylacenaphthene **2** was selectively obtained. The oxidation of **2** gave the corresponding naphthalic anhydride **3**, the reaction of which with hydroxylamine leads to the target 5,8-di-*tert*-butyl-*N*-hydroxynaphthalimide **4**. The total yield of the desired product for 3 stages was 48%.

2.2. Physical and Chemical Properties of 5,8-Di-*tert*-butyl-2-hydroxy-1*H*-benzo[de]isoquinoline-1,3(2*H*)-dione

The solubility of 5,8-di-*tert*-butyl-2-hydroxy-1*H*-benzo[de]isoquinoline-1,3(2*H*)-dione **4** was measured at room temperature (23–25 °C) in dichloromethane (DCM). It turned out that the solubility of the synthesized compound is 50 mg/mL, exceeding that for NHPI (ca. 1 mg/mL under the same conditions) by 50 times. Thus, we achieved the goal of obtaining *N*-hydroxyimide with high solubility in low-polarity medium.

At the next step, we studied the ability of **4** to generate a radical from *N*-oxyl radical upon oxidation in comparison with unsubstituted NHNI **6** (Scheme 2). The determination of absolute radical concentrations was carried out by quantitative EPR measurement using (4-Benzoyl-2,2,6,6-Tetramethylpiperidin-1-yl)oxyl (BzOTEMPO) as an external standard. Imide-*N*-oxyl radicals **5** and **7** were generated from equivalent amounts of the corresponding *N*-hydroxyimides (**4** or **6**, respectively) and lead tetraacetate Pb(OAc)₄ in acetonitrile (MeCN) at temperature 28 ± 1 °C and starting concentration of *N*-hydroxyimide 0.01 M.

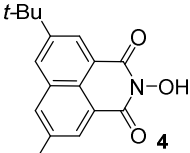
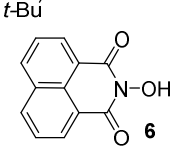
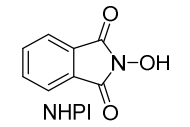
The obtained data showed that the synthesized di-*tert*-butyl-naphthalimide-*N*-oxyl radical **5** was slightly more stable than the unsubstituted naphthalimide-*N*-oxyl radical **7**. Both radicals have very similar *g*-factors (2.0068 for di-*tert*-butyl naphthalimide-*N*-oxyl radical **5** and 2.0069 for naphthalimide-*N*-oxyl radical **7**) and hyperfine coupling constants a_N (0.43 mT for both **5** and **7**).



Scheme 2. Generation of imide-*N*-oxyl radicals **5** and **7** from *N*-hydroxyimides **4** or **6**, EPR spectra of radicals **5** and **7**, and their decay curves according to quantitative EPR measurement.

In order to estimate the reactivity of di-*tert*-butyl-naphthalimide-*N*-oxyl radical **5** in hydrogen atom abstraction reactions, the NO-H BDE value for di-*tert*-butyl-*N*-hydroxynaphthalimide **4** was calculated on $\omega\text{B97M-D3BJ}/\text{def2-TZVPP}$ level of theory and compared with NO-H BDE values for unsubstituted NHNI **6** and most widely used *N*-hydroxyimide organocatalyst NHPI (Table 1). DFT methods are known to predict relative BDEs better than absolute BDEs [30]. Therefore, the isodesmic work reactions scheme was used for BDE calculations using the accurate experimental value of gas phase O-H BDE for H_2O as the reference (118.81 kcal/mol [31]). The calculated BDE values for NHPI and NHNI **6** are in good agreement with the literature data. It was found that NO-H BDE for di-*tert*-butyl-*N*-hydroxynaphthalimide **4** is almost equal to that of NHNI **6** (92.5 and 92.8 kcal/mol, respectively) and one of the highest in series of *N*-hydroxyimides making di-*tert*-butyl-naphthalimide-*N*-oxyl **5** very strong hydrogen abstracting agent comparable to naphthalimide-*N*-oxyl **7**. For example, NHPI demonstrates significantly lower NO-H BDE (by about 6 kcal/mol).

Table 1. The calculated NO-H BDE values for di-*tert*-butyl-*N*-hydroxynaphthalimide **4**, *N*-hydroxynaphthalimide **6** and *N*-hydroxyphthalimide (NHPI).

Structure	O–H BDE, kcal/mol ¹	Lit. O–H BDE Values
	92.5	-
	92.8	87.6 [26,32] ²
	86.5	88.1 [32] ³ 81.2 [26,32] ²

¹ Calculated for gas phase at ω B97M-D3BJ/def2-TZVPP level of theory employing isodesmic work reactions based on the recommended experimental value of O–H BDE in H₂O (118.81 kcal/mol [31]). ² According to DFT calculations. ³ Experimental values by EPR radical equilibration technique in *t*-BuOH.

3. Materials and Methods

3.1. General

In all experiments RT stands for 23–25 °C. Acenaphthene (99%), AlCl₃ anhydrous (99%), *tert*-butyl chloride (99%), sodium dichromate (99.5%), NaHCO₃ (99%), NH₂OH × HCl (99%), 4-Benzoyloxy-2,2,6,6-tetramethyl-piperidine-1-oxyl (BzOTEMPO, 97%) from commercial sources were used as is. MeCN was distilled over P₂O₅, CH₂Cl₂ was distilled over CaH₂. AcOH, EtOH were used as is from commercial sources. ¹H and ¹³C NMR spectra were recorded on a Bruker AVANCE II 300 and Bruker Fourier 300HD (300.13 and 75.47 MHz, respectively) spectrometers in CDCl₃. The residual signal of CHCl₃ in CDCl₃ (7.26 ppm) was used as a chemical shift reference in ¹H NMR spectra. The central line of CDCl₃ signal (77.16 ppm) was used as a chemical shift reference in ¹³C NMR spectra. FT-IR spectra were recorded on Bruker Alpha instrument. IR spectra were registered in KBr pellets for solid compounds, and liquid compounds were placed between two KBr windows to make a thin layer. High resolution mass spectra (HR-MS) were measured on a Bruker maXis instrument using electrospray ionization (ESI). The measurements were performed in a positive ion mode (interface capillary voltage—4500 V); mass range from *m/z* 50 to *m/z* 3000 Da; external calibration with Electrospray Calibrant Solution (Fluka Analytical/Sigma Aldrich, Buchs, Switzerland). A syringe injection was used for all acetonitrile solutions (flow rate 3 μL/min). Nitrogen was applied as a dry gas; interface temperature was set at 180 °C. EPR spectra were recorded on X-band spectrometer Adani Spinscan X. General conditions of EPR measurements: center field—336.12 mT, sweep width—15 mT, sweep time—60 s, modulation amplitude—100 μT, temperature—28 ± 1 °C. Quantitative results were obtained using 4-Benzoyloxy-2,2,6,6-tetramethyl-piperidine-1-oxyl (BzOTEMPO) as an external standard: three EPR spectra were recorded from the solution 0.01 M BzOTEMPO in MeCN and results were averaged and then used for further calculations. Concentrations of imide-*N*-oxyl radicals were calculated from equation:

$$C_{\text{radical}} = C_{\text{BzOTEMPO}} \frac{I_{\text{radical}}}{I_{\text{BzOTEMPO}}} \quad (1)$$

where C_{radical} —concentration of radical **5** or **7**, M, I_{radical} —double integrals of corresponding EPR signals of radical **5** or **7**, I_{BzOTEMPO} —double integral of EPR signal of reference BzOTEMPO solution in MeCN with BzOTEMPO concentration = C_{BzOTEMPO} .

3.2. Experimental Details for the Scheme 1

The 5,8-di-*tert*-butyl-2-hydroxy-1*H*-benzo[de]isoquinoline-1,3(2*H*)-dione **4** was synthesized according to the modified methods described previously [29,33–35]. Anhydrous aluminum chloride (0.41 mmol, 56 mg) was added during 1 h to a stirred solution of acenaphthene **1** (20.00 mmol, 3.084 g) and *tert*-butyl chloride (44.12 mmol, 4.085 g) in dry CH₂Cl₂ (10 mL). The mixture was refluxed for 2 h then left to stir for a further 24 h at room temperature. The reaction mixture was quenched with water (20 mL). The water layer was extracted with CH₂Cl₂ (3 × 20 mL). All organic extracts were combined, and the solvent was removed under reduced pressure. The crude product was recrystallized from EtOH to obtain **2** as orange needles (4.16 g, 15.6 mmol, 78%). ¹H NMR (300 MHz, Chloroform-*d*) δ 7.62–7.55 (m, 2H), 7.42–7.38 (m, 2H), 3.43 (s, 4H), 1.47 (s, 18H). ¹³C{¹H}NMR (75.48 MHz, CDCl₃) δ 151.4, 145.2, 136.4, 130.9, 117.6, 117.5, 35.5, 31.8, 30.7.

To a solution of **2** (4.16 g, 15.6 mmol) in acetic acid (60 mL), sodium dichromate (11.17 g, 40.0 mmol) was added with stirring at room temperature. The suspension was heated at 75 °C for 8 h. After the completion of the reaction, cold water was added to the reaction mixture to get solid, which was filtered and washed with water. Slightly yellow anhydride **3** (3.05 g, 9.8 mmol, 63%) was obtained. ¹H NMR (300 MHz, Chloroform-*d*) δ 8.64 (d, *J* = 1.7 Hz, 2H), 8.23 (d, *J* = 1.7 Hz, 2H), 1.48 (s, 18H). ¹³C{¹H}NMR (75.48 MHz, CDCl₃) δ 161.2, 151.1, 132.3, 131.5, 130.8, 127.2, 118.4, 35.4, 31.2. The spectral data of **3** are consistent with previously reported [36].

Anhydride **3** (3.05 g, 9.8), NaHCO₃ (1.26 g, 15 mmol), NH₂OH × HCl (1.04 g, 15 mmol) and EtOH (100 mL) were placed in a 250 mL round-bottomed flask. The mixture was refluxed for 2.5 h, then the solvent was evaporated and the residue was diluted with CH₂Cl₂ (50 mL) and water (50 mL). The layers were shaken, and organic phase was separated. The water layer was extracted with CH₂Cl₂ (2 × 50 mL). All organic extracts were combined, dried over MgSO₄, and the solvent was rotary evaporated. The desired product **4** was obtained as yellow needle crystals (3.08 g, 9.5 mmol, 97%). Mp = 198–199 °C (lit. Mp = 180 °C [35]). ¹H NMR (300 MHz, Chloroform-*d*) δ 8.68 (d, *J* = 1.8 Hz, 2H), 8.17 (d, *J* = 1.8 Hz, 2H), 1.47 (s, 18H). ¹³C{¹H}NMR (75.48 MHz, CDCl₃) δ 160.0, 150.8, 132.3, 130.6, 130.1, 123.3, 121.1, 35.5, 31.3. FTIR (KBr): ν_{max} = 3510, 3158, 2964, 2906, 2871, 1707, 1681, 1652, 1629, 1601, 1476, 1429, 1395, 1366, 1320, 1230, 1207, 1057, 912, 892, 798, 730, 627 cm⁻¹. HR-MS (ESI): *m/z* = 326.1748, calcd. for C₂₀H₂₃NO₃ + nH⁺: 326.1751. Copies of spectra are presented in Supplementary Materials.

3.3. Experimental Method for the Solubility Measuring of NHPI and **4**

An excess amount of *N*-hydroxyimide (NHPI or **4**) was dissolved in 10 mL of DCM at room temperature (23–25 °C) until a saturated solution was obtained. Then a 5 mL aliquot was taken, evaporated and the residue was weighed. Solubility was determined as the mass of the residue divided by the volume of solvent (5 mL).

3.4. Experimental Details for the Scheme 2

To a solution of **4** (0.1 mmol, 32.5 mg) in MeCN (10 mL) the Pb(OAc)₄ (0.05 mmol, 23.3 mg) was added. The resulting solution was thoroughly mixed, and EPR spectrum was recorded 2 min after the addition of oxidant. Subsequent spectra were recorded every 2 min.

3.5. Experimental Details for the Table 1 (Computational Details)

NO-H BDE values were calculated using isodesmic work reaction R₂NOH + •OH = R₂NO• + H₂O. Based on this isodesmic work reaction BDE_{NO-H} was calculated as H(R₂NO•) + H(H₂O) – H(R₂NOH) – H(•OH) + BDE_{H₂O}, where H are enthalpy values from DFT calculations and BDE_{H₂O} is the recommended precise experimental value of O–H BDE in H₂O (118.81 kcal/mol [31]). Geometry optimizations and thermochemical calculations were realized in Orca 5.03 software package [37,38], LibXC [39] implemented version of ωB97M-D3BJ exchange-correlation functional [40–43] with atom-pairwise dispersion

correction with the Becke–Johnson damping scheme (D3BJ) [44,45], and def2-TZVPP basis set [46]. Optimized structures were visualized using Avogadro 1.2.0 program [47]. All calculations were performed for temperature 298.15 K and pressure 1 atm. Atomic XYZ cartesian coordinates in optimized structures are presented in Supplementary Materials.

4. Conclusions

The 5,8-di-*tert*-butyl-*N*-hydroxynaphthalimide **4** was presented as a new lipophilic *N*-hydroxyimide with high solubility in organic medium with potential application as *N*-oxyl radical precursor for free-radical oxidative processes. Along with improved solubility in low-polarity solvents it demonstrates chemical characteristics similar to those of unsubstituted NHNI: similar self-decay profile and high NO–H BDE value. The high NO–H BDE (92.5 kcal/mol according to ω B97M-D3BJ/def2-TZVPP calculation) in **4** and relatively slow self-decay of the corresponding *N*-oxyl radical **5** make **4** perspective *N*-oxyl radical precursor for CH-functionalization of unactivated substrates by hydrogen atom abstraction.

Supplementary Materials: ^1H and ^{13}C NMR Spectra, FT-IR spectrum, HR-MS spectrum of 5,8-Di-*tert*-butyl-*N*-hydroxynaphthalimide **4**, optimized geometries of 5,8-Di-*tert*-butyl-*N*-hydroxynaphthalimide **4**, NHNI **6**, NHPI and the corresponding *N*-oxyl radicals used for calculation of NO–H BDE values.

Author Contributions: Conceptualization, I.B.K. and A.O.T.; investigation, I.B.K., A.D.K. and E.R.L.; writing—original draft preparation, E.R.L. and I.B.K.; writing—review and editing, I.B.K.; visualization, E.R.L.; supervision, I.B.K. and A.O.T.; project administration, I.B.K. and A.O.T. All authors have read and agreed to the published version of the manuscript.

Funding: This research received no external funding.

Data Availability Statement: Not applicable.

Conflicts of Interest: The authors declare no conflict of interest.

References

1. Tretyakov, E.V.; Ovcharenko, V.I.; Terent'ev, A.O.; Krylov, I.B.; Magdesieva, T.V.; Mazhukin, D.G.; Gritsan, N.P. Conjugated Nitroxides. *Russ. Chem. Rev.* **2022**, *91*, RCR5025. [[CrossRef](#)]
2. Recupero, F.; Punta, C. Free Radical Functionalization of Organic Compounds Catalyzed by *N*-Hydroxyphthalimide. *Chem. Rev.* **2007**, *107*, 3800–3842. [[CrossRef](#)] [[PubMed](#)]
3. Krylov, I.B.; Lopat'eva, E.R.; Subbotina, I.R.; Nikishin, G.I.; Yu, B.; Terent'ev, A.O. Mixed Hetero-/Homogeneous TiO_2 /*N*-Hydroxyimide Photocatalysis in Visible-Light-Induced Controllable Benzylic Oxidation by Molecular Oxygen. *Chin. J. Catal.* **2021**, *42*, 1700–1711. [[CrossRef](#)]
4. Andrade, M.A.; Martins, L.M.D.R.S. Organocatalysis Meets Hydrocarbon Oxyfunctionalization: The Role of *N*-Hydroxyimides. *Eur. J. Org. Chem.* **2021**, *2021*, 4715–4727. [[CrossRef](#)]
5. Gaster, E.; Kozuch, S.; Pappo, D. Selective Aerobic Oxidation of Methylarenes to Benzaldehydes Catalyzed by *N*-Hydroxyphthalimide and Cobalt(II) Acetate in Hexafluoropropan-2-ol. *Angew. Chem. Int. Ed.* **2017**, *56*, 5912–5915. [[CrossRef](#)]
6. Wang, L.; Zhang, Y.; Du, R.; Yuan, H.; Wang, Y.; Yao, J.; Li, H. Selective One-Step Aerobic Oxidation of Cyclohexane to ϵ -Caprolactone Mediated by *N*-Hydroxyphthalimide (NHPI). *ChemCatChem* **2019**, *11*, 2260–2264. [[CrossRef](#)]
7. Goncharova, I.K.; Tukhvatshin, R.S.; Novikov, R.A.; Volodin, A.D.; Korlyukov, A.A.; Lakhtin, V.G.; Arzumanyan, A.V. Complementary Cooperative Catalytic Systems in the Aerobic Oxidation of a Wide Range of Si–H-Reagents to Si–OH-Products: From Monomers to Oligomers and Polymers. *Eur. J. Org. Chem.* **2022**, *2022*, e202200871. [[CrossRef](#)]
8. Krylov, I.B.; Paveliev, S.A.; Budnikov, A.S.; Segida, O.O.; Merkulova, V.M.; Vil', V.A.; Nikishin, G.I.; Terent'ev, A.O. Hidden Reactivity of Barbituric and Meldrum's Acids: Atom-Efficient Free-Radical C–O Coupling with *N*-Hydroxy Compounds. *Synthesis* **2022**, *54*, 506–516. [[CrossRef](#)]
9. Krylov, I.B.; Paveliev, S.A.; Shelimov, B.N.; Lokshin, B.V.; Garbuzova, I.A.; Tafenko, V.A.; Chernyshev, V.V.; Budnikov, A.S.; Nikishin, G.I.; Terent'ev, A.O. Selective Cross-Dehydrogenative C–O Coupling of *N*-Hydroxy Compounds with Pyrazolones. Introduction of the Diacetyliminoxyl Radical into the Practice of Organic Synthesis. *Org. Chem. Front.* **2017**, *4*, 1947–1957. [[CrossRef](#)]
10. Terent'ev, A.O.; Krylov, I.B.; Timofeev, V.P.; Starikova, Z.A.; Merkulova, V.M.; Ilovaisky, A.I.; Nikishin, G.I. Oxidative C–O Cross-Coupling of 1,3-Dicarbonyl Compounds and Their Heteroanalogues with *N*-Substituted Hydroxamic Acids and *N*-Hydroxyimides. *Adv. Synth. Catal.* **2013**, *355*, 2375–2390. [[CrossRef](#)]

11. Terent'ev, A.O.; Krylov, I.B.; Sharipov, M.Y.; Kazanskaya, Z.M.; Nikishin, G.I. Generation and Cross-Coupling of Benzyl and Phthalimide-*N*-Oxyl Radicals in a Cerium(IV) Ammonium Nitrate/*N*-Hydroxyphthalimide/ArCH₂R System. *Tetrahedron* **2012**, *68*, 10263–10271. [[CrossRef](#)]
12. Krylov, I.B.; Lopat'eva, E.R.; Budnikov, A.S.; Nikishin, G.I.; Terent'ev, A.O. Metal-Free Cross-Dehydrogenative C–O Coupling of Carbonyl Compounds with *N*-Hydroxyimides: Unexpected Selective Behavior of Highly Reactive Free Radicals at an Elevated Temperature. *J. Org. Chem.* **2020**, *85*, 1935–1947. [[CrossRef](#)] [[PubMed](#)]
13. Dai, P.-F.; Wang, Y.-P.; Qu, J.-P.; Kang, Y.-B. *Tert*-Butyl Nitrite as a Twofold Hydrogen Abstractor for Dehydrogenative Coupling of Aldehydes with *N*-Hydroxyimides. *Org. Lett.* **2021**, *23*, 9360–9364. [[CrossRef](#)] [[PubMed](#)]
14. Feizpour, F.; Jafarpour, M.; Rezaeifard, A. A Photoinduced Cross-Dehydrogenative-Coupling (CDC) Reaction between Aldehydes and *N*-Hydroxyimides by a TiO₂–Co Ascorbic Acid Nanohybrid under Visible Light Irradiation. *New J. Chem.* **2018**, *42*, 807–811. [[CrossRef](#)]
15. Zhang, M.-Z.; Luo, N.; Long, R.-Y.; Gou, X.-T.; Shi, W.-B.; He, S.-H.; Jiang, Y.; Chen, J.-Y.; Chen, T. Transition-Metal-Free Oxidative Aminooxyarylation of Alkenes: Annulations toward Aminooxylated Oxindoles. *J. Org. Chem.* **2018**, *83*, 2369–2375. [[CrossRef](#)]
16. Bhardwaj, M.; Grover, P.; Rasool, B.; Mukherjee, D. Recent Advances in *N*-Hydroxyphthalimide: As a Free Radical Initiator and Its Applications. *Asian J. Org. Chem.* **2022**, *11*, 442. [[CrossRef](#)]
17. LaMartina, K.B.; Kuck, H.K.; Oglesbee, L.S.; Al-Odaini, A.; Boaz, N.C. Selective Benzylic C–H Monooxygenation Mediated by Iodine Oxides. *Beilstein J. Org. Chem.* **2019**, *15*, 602–609. [[CrossRef](#)]
18. Xia, X.-F.; Zhu, S.-L.; Zhang, D. Copper-Catalyzed C–O Coupling of Styrenes with *N*-Hydroxyphthalimide through Dihydroxylation Reactions. *Tetrahedron* **2015**, *71*, 8517–8520. [[CrossRef](#)]
19. Krylov, I.B.; Paveliev, S.A.; Matveeva, O.K.; Terent'ev, A.O. Cerium(IV) Ammonium Nitrate: Reagent for the Versatile Oxidative Functionalization of Styrenes Using *N*-Hydroxyphthalimide. *Tetrahedron* **2019**, *75*, 2529–2537. [[CrossRef](#)]
20. Paveliev, S.A.; Segida, O.O.; Dvoretzkiy, A.; Dzyunov, M.M.; Fedorova, U.V.; Terent'ev, A.O. Electrifying Phthalimide-*N*-Oxyl (PINO) Radical Chemistry: Anodically Induced Dioxygenation of Vinyl Arenes with *N*-Hydroxyphthalimide. *J. Org. Chem.* **2021**, *86*, 18107–18116. [[CrossRef](#)]
21. Petroselli, M.; Melone, L.; Cametti, M.; Punta, C. Lipophilic *N*-Hydroxyphthalimide Catalysts for the Aerobic Oxidation of Cumene: Towards Solvent-Free Conditions and Back. *Chem. Eur. J.* **2017**, *23*, 10616–10625. [[CrossRef](#)] [[PubMed](#)]
22. Sawatari, N.; Yokota, T.; Sakaguchi, S.; Ishii, Y. Alkane Oxidation with Air Catalyzed by Lipophilic *N*-Hydroxyphthalimides without Any Solvent. *J. Org. Chem.* **2001**, *66*, 7889–7891. [[CrossRef](#)]
23. Petroselli, M.; Franchi, P.; Lucarini, M.; Punta, C.; Melone, L. Aerobic Oxidation of Alkylaromatics Using a Lipophilic *N*-Hydroxyphthalimide: Overcoming the Industrial Limit of Catalyst Solubility. *ChemSusChem* **2014**, *7*, 2695–2703. [[CrossRef](#)] [[PubMed](#)]
24. Kushch, O.V.; Hordieieva, I.O.; Kompanets, M.O.; Zosenko, O.O.; Opeida, I.A.; Shendrik, A.N. Hydrogen Atom Transfer from Benzyl Alcohols to *N*-Oxyl Radicals. Reactivity Parameters. *J. Org. Chem.* **2021**, *86*, 3792–3799. [[CrossRef](#)]
25. Yoshii, T.; Tsuzuki, S.; Sakurai, S.; Sakamoto, R.; Jiang, J.; Hatanaka, M.; Matsumoto, A.; Maruoka, K. *N*-Hydroxybenzimidazole as a Structurally Modifiable Platform for *N*-Oxyl Radicals for Direct C–H Functionalization Reactions. *Chem. Sci.* **2020**, *11*, 5772–5778. [[CrossRef](#)] [[PubMed](#)]
26. Toribio, P.P.; Gimeno-Gargallo, A.; Capel-Sanchez, M.C.; de Frutos, M.P.; Campos-Martin, J.M.; Fierro, J.L.G. Ethylbenzene Oxidation to Its Hydroperoxide in the Presence of *N*-Hydroxyimides and Minute Amounts of Sodium Hydroxide. *Appl. Catal. A Gen.* **2009**, *363*, 32–39. [[CrossRef](#)]
27. Shibamoto, A.; Sakaguchi, S.; Ishii, Y. Aerobic Oxidation of Ethane to Acetic Acid Catalyzed by *N,N'*-Dihydroxypyromellitimide Combined with Co Species. *Tetrahedron Lett.* **2002**, *43*, 8859–8861. [[CrossRef](#)]
28. Kishioka, S. Electrocatalytic Kinetics of *N*-Hydroxynaphthalimide as a Redox Mediator for Benzyl Alcohol Oxidation Using Rotating Disk Electrode Voltammetry. *Electrocatalysis* **2022**, *13*, 210–217. [[CrossRef](#)]
29. Altieri, A.; Gatti, F.G.; Kay, E.R.; Leigh, D.A.; Martel, D.; Paolucci, F.; Slawin, A.M.Z.; Wong, J.K.Y. Electrochemically Switchable Hydrogen-Bonded Molecular Shuttles. *J. Am. Chem. Soc.* **2003**, *125*, 8644–8654. [[CrossRef](#)]
30. Feng, Y.; Liu, L.; Wang, J.-T.; Huang, H.; Guo, Q.-X. Assessment of Experimental Bond Dissociation Energies Using Composite Ab Initio Methods and Evaluation of the Performances of Density Functional Methods in the Calculation of Bond Dissociation Energies. *J. Chem. Inf. Comput. Sci.* **2003**, *43*, 2005–2013. [[CrossRef](#)]
31. Luo, Y.-R. *Handbook of Bond Dissociation Energies in Organic Compounds*; CRC Press: Boca Raton, FL, USA, 2003; ISBN 978-0-8493-1589-3.
32. Hermans, I.; Jacobs, P.; Peeters, J. Autoxidation Catalysis with *N*-Hydroxyimides: More-Reactive Radicals or Just More Radicals? *Phys. Chem. Chem. Phys.* **2007**, *9*, 686. [[CrossRef](#)] [[PubMed](#)]
33. Verma, M.; Luxami, V.; Paul, K. Synthesis, in Vitro Evaluation and Molecular Modelling of Naphthalimide Analogue as Anticancer Agents. *Eur. J. Med. Chem.* **2013**, *68*, 352–360. [[CrossRef](#)] [[PubMed](#)]
34. Kushch, O.; Hordieieva, I.; Novikova, K.; Litvinov, Y.; Kompanets, M.; Shendrik, A.; Opeida, I. Kinetics of *N*-Oxyl Radicals' Decay. *J. Org. Chem.* **2020**, *85*, 7112–7124. [[CrossRef](#)] [[PubMed](#)]
35. Peters, A.T. 110. Acenaphthene Series. Part I. Mono- and Di-*Tert*-Butyl-Acenaphthene, -Acenaphthenequinone, and -Naphthalic Anhydride, and Their Derivatives. *J. Chem. Soc.* **1942**, 562–565. [[CrossRef](#)]

36. Ragazzon, G.; Credi, A.; Colasson, B. Thermodynamic Insights on a Bistable Acid-Base Switchable Molecular Shuttle with Strongly Shifted Co-Conformational Equilibria. *Chem. Eur. J.* **2017**, *23*, 2149–2156. [[CrossRef](#)]
37. Neese, F. Software Update: The ORCA Program System—Version 5.0. *WIREs Comput. Mol. Sci.* **2022**, *12*, 1606. [[CrossRef](#)]
38. Neese, F. Software Update: The ORCA Program System, Version 4.0. *WIREs Comput. Mol. Sci.* **2018**, *8*, 1327. [[CrossRef](#)]
39. Lehtola, S.; Steigemann, C.; Oliveira, M.J.T.; Marques, M.A.L. Recent Developments in Libxc—A Comprehensive Library of Functionals for Density Functional Theory. *SoftwareX* **2018**, *7*, 1–5. [[CrossRef](#)]
40. Mardirossian, N.; Head-Gordon, M. ω B97M-V: A Combinatorially Optimized, Range-Separated Hybrid, Meta-GGA Density Functional with VV10 Nonlocal Correlation. *J. Chem. Phys.* **2016**, *144*, 214110. [[CrossRef](#)]
41. Mardirossian, N.; Head-Gordon, M. Mapping the Genome of Meta-Generalized Gradient Approximation Density Functionals: The Search for B97M-V. *J. Chem. Phys.* **2015**, *142*, 074111. [[CrossRef](#)]
42. Najibi, A.; Goerigk, L. The Nonlocal Kernel in van Der Waals Density Functionals as an Additive Correction: An Extensive Analysis with Special Emphasis on the B97M-V and Ω B97M-V Approaches. *J. Chem. Theory Comput.* **2018**, *14*, 5725–5738. [[CrossRef](#)] [[PubMed](#)]
43. Najibi, A.; Goerigk, L. DFT-D4 Counterparts of Leading META-Generalized-gradient Approximation and Hybrid Density Functionals for Energetics and Geometries. *J. Comput. Chem.* **2020**, *41*, 2562–2572. [[CrossRef](#)] [[PubMed](#)]
44. Grimme, S.; Ehrlich, S.; Goerigk, L. Effect of the Damping Function in Dispersion Corrected Density Functional Theory. *J. Comput. Chem.* **2011**, *32*, 1456–1465. [[CrossRef](#)]
45. Grimme, S.; Antony, J.; Ehrlich, S.; Krieg, H. A Consistent and Accurate Ab Initio Parametrization of Density Functional Dispersion Correction (DFT-D) for the 94 Elements H-Pu. *J. Chem. Phys.* **2010**, *132*, 154104. [[CrossRef](#)] [[PubMed](#)]
46. Weigend, F.; Ahlrichs, R. Balanced Basis Sets of Split Valence, Triple Zeta Valence and Quadruple Zeta Valence Quality for H to Rn: Design and Assessment of Accuracy. *Phys. Chem. Chem. Phys.* **2005**, *7*, 3297. [[CrossRef](#)] [[PubMed](#)]
47. Hanwell, M.D.; Curtis, D.E.; Lonie, D.C.; Vandermeersch, T.; Zurek, E.; Hutchison, G.R. Avogadro: An Advanced Semantic Chemical Editor, Visualization, and Analysis Platform. *J. Cheminform.* **2012**, *4*, 17. [[CrossRef](#)]

Disclaimer/Publisher's Note: The statements, opinions and data contained in all publications are solely those of the individual author(s) and contributor(s) and not of MDPI and/or the editor(s). MDPI and/or the editor(s) disclaim responsibility for any injury to people or property resulting from any ideas, methods, instructions or products referred to in the content.